

THREE-DIMENSIONAL DIGITAL HALFTONING FOR LAYERED MANUFACTURING BASED ON DROPLETS

Chi Zhou and Yong Chen
Epstein Department of Industrial and Systems Engineering
University of Southern California
Los Angeles, California

KEYWORDS

Digital Halftoning, Layered Manufacturing, Droplet Planning, Multi-Jet Modeling, Polyjet.

ABSTRACT

Layered manufacturing based on droplets, such as multi-jet modeling and polyjet processes, shows great promises in fabricating accurate, smooth and highly detailed 3-dimensional models. It has been widely used in fabricating prototypes and investment casting patterns. In this paper, we present a 3-dimensional digital halftoning method which can significantly reduce the building time of these layered manufacturing processes. The key idea of the halftoning method is to intelligently control the printed droplet layout to form a slanted layer, which can closely match the surface of an input geometry. We present a mathematical model for finding the optimized droplet layout, and discuss various solution strategies. The experimental results showed that a revised DBS method can solve the formulated problem effectively and efficiently.

1. INTRODUCTION

Layered manufacturing (LM) based on additive principle can fabricate parts directly from CAD

models without part-specific tooling or fixturing. During the last two decades, many novel LM processes have been developed by using a wide variety of technologies. In this paper, we are interested in the LM processes that are based on droplets. That is, a solid object is formed by selectively spraying droplets of melted liquid material that then solidify into a layer. Since the droplet spraying is mostly based on the inkjet technology, we will call these processes *inkjet printing*. Two of such processes are *multi-jet modeling* (such as *InVision* and *ProJet* from *3D Systems Inc.*) and *Polyjet* (such as *Eden* and *Connex* from *Objet Geometries*). These systems can build accurate, smooth and highly detailed 3-dimensional models, and have been widely used in fabricating prototypes and investment casting patterns for applications such as jewelry.

As shown in Figure 1, currently a uniform slicing scheme is used in the inkjet printing processes, in which a set of uniform horizontal planes are constructed to intersect the CAD model. An intersected planar contour is then converted into a layer image which will be used to approximate the related layer i . Uniform hatch patterns can also be used. Based on the approach, an approximation error is proportional to the layer thickness that was used in slicing. Hence an ultra-thin layer thickness is required to ensure an accurate approximation and smooth surface finish (e.g. 0.016mm is used for *Eden*

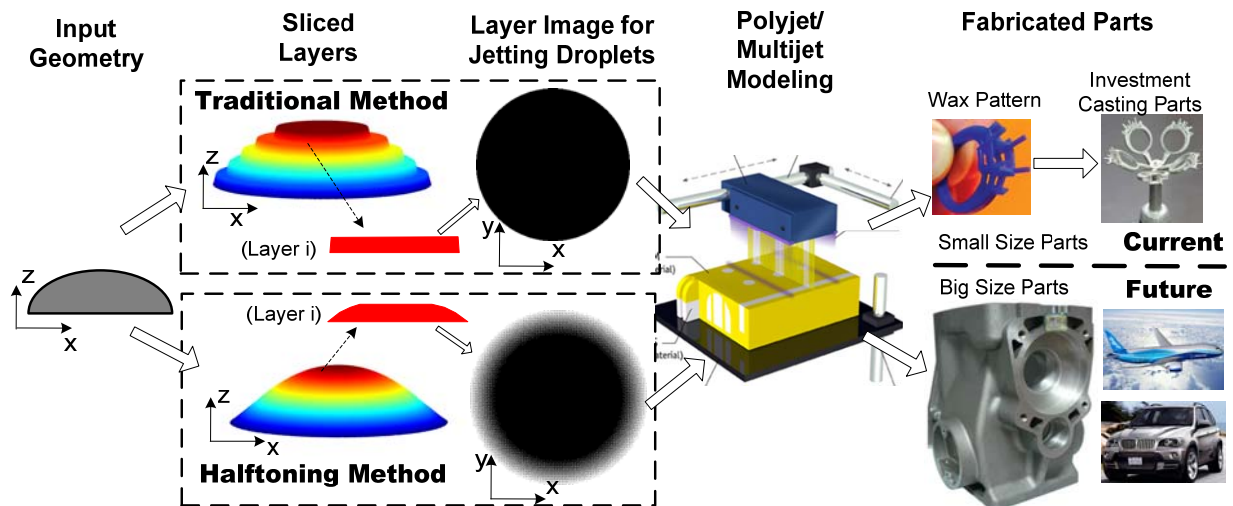


FIGURE 1. COMPARISON BETWEEN TRADITIONAL METHOD AND HALFTONING METHOD.

and 0.032mm is used for *InVision* machines). However, the ultra-thin layers will also significantly slow down the building process. For example, to build a part that is 500 mm high, it will require 31,250 layers for a layer thickness at 0.016 mm, or 130 hours if each layer takes 15 second. Such extremely long building time severely limits the usage of inkjet printing for big size parts such as investment casting patterns for automobile or aerospace applications.

In this paper, we present a 3-dimensional digital halftoning method for the inkjet printing processes. It allows the uniform slicing scheme to utilize a much bigger layer thickness without sacrificing the approximation accuracy. The key idea of the digital halftoning method is to intelligently control the jetting of droplets to form a slanted layer which can closely match the surface of an input geometry (refer to a comparison in Figure 1). We illustrate that, based on the technique, we can have a small approximation error by using a layer thickness that is 8 times bigger (refer to the Section 6.1). Therefore, we can significantly reduce the required layer number and, consequently, the building time in the inkjet printing processes. The technical contributions of this paper are: (1) we present a unique approach for reducing the building time of inkjet printing processes; (2) we develop a systematic method for generating optimized droplet layout; and (3) we identify an effective and efficient solution strategy for the formulated problem.

2. RELATED WORK

Part slicing including uniform slicing, adaptive slicing, and direct slicing have been extensively studied for layered manufacturing processes. However, all the work focused on the calculation of intersections between parallel horizontal planes with a CAD or STL model. Many different approaches for achieving a slanted layer have also been presented. Kulkarni [1] used 3-Axis CNC machining to post-process 2D layers; Hope et al. [2] used a water-jet cutter to finish 2D layers; Amon et al. [3] used 5-axis CNC machining in their shape deposition process; Khoshnevis [4] used trowel in the Contour Crafting process; Horvath and Vergeest [5] used a flexible and curved cutting tool to cut soft material in the Thick Layer Object Manufacturing process. In this paper, we will use digital halftoning technique to intelligently deposit droplets into a slanted layer. No post-processing processes are required.

In 2D printing industry, digital halftoning techniques have been widely adopted [6]. To print a continuous-tone image by using bi-level devices such as inkjet printers, the gray scale image must be transformed into a binary image (i.e. 0/1). The 2D digital halftoning techniques relies on the fact that the human eyes act as special low-pass filter and perceive the binary texture patterns as continuous tones at normal viewing distances. Generally, digital halftoning algorithms can be grouped into three categories: (1) screening, also called dithering, such as the dispersed dot screen introduced by Bayer [7]; (2) error diffusion such as Floyd and Steinberg algorithm [8]; and (3) optimization methods by iteratively scanning the original image to minimize the perceived error, such as the iterative direct binary search (DBS) algorithm [9].

3. PRINCIPLE OF INKJET PRINTING

Although all based on the inkjet technology, the *inkjet printing* is different from *3D printing* in that, jetted droplets of a material (such as wax or thermoplastic) will be accumulated in the *inkjet printing* process to form a layer; while adhesive droplets are jetted to selectively bond layers of fine powders in the *3D printing* process (such as *ZPrinter* from *Z Corporation*). Therefore the principle of our approach for *inkjet printing* is different from that of the local composition control developed for *3D printing* [10].

Most inkjet printers use a piezoelectric material in a liquid-filled chamber behind each nozzle (refer to Figure 2-right). When a voltage is applied, the piezoelectric material changes shape or size, which generates a pressure pulse in the fluid forcing a droplet from the nozzle. The droplet jetting, forming and impacting on a surface involve complicated and intriguing physics. They have been extensively studied in the 2-Dimensional inkjet printing industry. As shown in [11], after jetted onto a surface, an ink droplet is in the shape of a half ellipsoid due to capillary effects (refer to Figure 2). A similar shape has been confirmed for a droplet of hydrophilic conductive polymer [12]. In this paper, we will use function $h(x, y)$ to represent the shape of a droplet in forming a layer. We further assume $h(x, y)$ is in the shape of a half ellipsoid whose parameters can be estimated from the volume of a droplet. Therefore, the principle of inkjet printing is to control the convolution of jetted droplets to selectively form a layer.

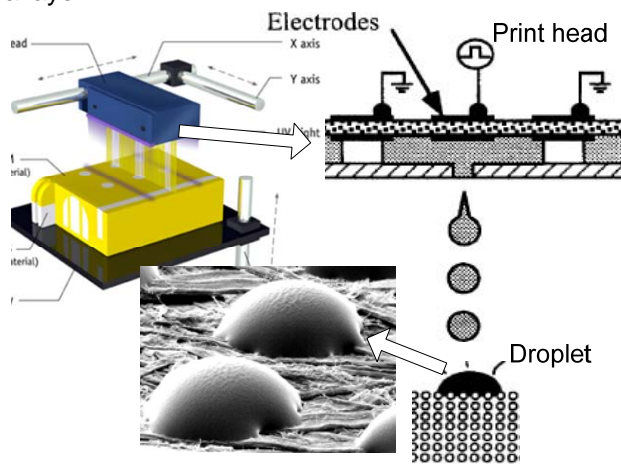


FIGURE 2. PRINCIPLE OF INKJET PRINTING.

Similar to a 2D inkjet printer, a 3D inkjet printer is also a bi-level device, which can only determine whether to print a droplet at any

moment. Typically the print heads can move in both X and Y directions to cover the building platform (refer to Figure 2-left). Determined by the minimum resolution of a related step motor, the XY resolution is usually much smaller than the size of a droplet. Therefore, a challenging problem for the halftoning method is to determine when to print droplets. Conceptually, based on the XY resolution, we can construct a binary bitmap for the print head controller such that it will print droplets at all the pixels assigned "1" and skip all other pixels. After finishing a layer, all the jetted droplets will accumulate together to form the desired shape of the layer. In the rest of the paper, we will present a mathematical model and related solution strategies for identifying such an optimized droplet layout.

4. PROBLEM FORMULATION

Based on the principle of inkjet printing, we mathematically define the digital halftoning problem as follows. For a specific layer i , we denote $c(x, y)$ as the ratio of the Z -height at the location (x, y) to the layer thickness (refer to Figure 3). So $c(x, y)$ is a continuous tone and $c(x, y) \in [0, 1]$. We sample the continuous surface according to a given XY resolution. For each sampling point (m, n) , we have a bi-level signal $b(m, n)$, such that $b(m, n) = 1$ represents printing a droplet at (m, n) , otherwise skipping the point. A printed droplet spreads out by a shape function $h(x, y)$, and convoluted with other droplets if they are overlapped. We denote the convoluted result at (x, y) as $a(x, y)$. Hence we get the objective value \mathcal{E} by summing all the mean squared error (MSE) between $a(x, y)$ and $c(x, y)$. Our aim is to generate a halftone image b to reduce the error as small as possible. The problem can be formulated as follows:

$$\mathcal{E} = \int_0^W \int_0^H |e(x, y)|^2 dx dy \quad (1)$$

where W and H denote the width and the height of the layer respectively. $e(x, y)$ denotes the error between the convoluted result and the given ratio in the continuous space, which is formulated as follows:

$$e(x, y) = a(x, y) - c(x, y) \quad (2)$$

In practice, we can use the discrete summation to approximate the integration in Equation (1) as:

$$\mathcal{E} \approx \sum_{p=0}^{NW} \sum_{q=0}^{NH} |e(p, q)|^2 \quad (3)$$

The convoluted result $a(x, y)$ at point (x, y) is:

$$a(x, y) = (b \otimes h)(x, y) = \sum_{m=0}^{NW} \sum_{n=0}^{NH} b(m, n) \cdot h(x - m\omega, y - n\omega) \quad (4)$$

Where \otimes denotes convolution operator, ω denotes the pixel width, $NW \times NH$ is the number of pixels of the halftone signal. h denotes the convolution function. For the shape of a half ellipsoid, we know:

$$h(x, y) = \begin{cases} \delta_z \sqrt{1 - \frac{x^2}{\delta_x^2} - \frac{y^2}{\delta_y^2}} & \frac{x^2}{c\omega^2} + \frac{y^2}{ch^2} \leq 1 \\ 0 & \text{otherwise} \end{cases} \quad (5)$$

The parameter values, $\delta_x, \delta_y, \delta_z$, can be estimated according to the technique specifications of a print head.

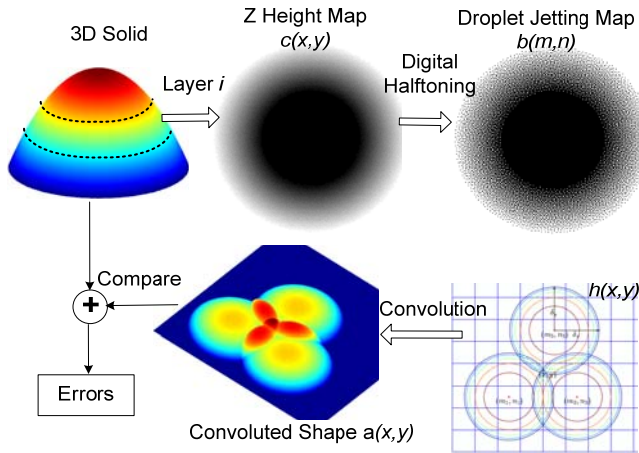


FIGURE 3. ILLUSTRATION OF HALFTONING PROBLEM.

5. COMPUTATIONAL STRATEGIES

An effective and efficient computational method for the formulated halftoning problem is essential since a halftoning image may have a large number of pixels (over 10,000 x 10,000 pixels). In this section, we present our investigation of various digital halftoning algorithms for the layered manufacturing application.

5.1 Mixed Integer Programming Model. We first formulate a quadratic integer optimization

model, whose solution can give us the global optimum of the droplet layout.

$$\begin{aligned} & \underset{b}{\text{minimize}} \quad \sum_{p=1}^{NW} \sum_{q=1}^{NH} |a(p, q) - c(p, q)|^2 \\ & \text{s.t.} \quad b \in \{0, 1\} \\ & \text{wherea} \quad (p, q) = \sum_{(m, n) \in S^{pq}} G_{mn}(p, q) \cdot b(m, n) \end{aligned} \quad (6)$$

$$S^{pq} = \left\{ (m, n) \left| \frac{(p-m)^2}{c\omega^2} + \frac{(q-n)^2}{ch^2} \leq 1 \right. \right\}$$

$$G_{x_0, y_0}(x, y) = \delta_z \sqrt{1 - \frac{(x-x_0)^2}{\delta_x^2} - \frac{(y-y_0)^2}{\delta_y^2}}$$

Even though this problem has convex quadratic objective, it is NP-hard. In practice, solving this problem to optimality can be extremely difficult when there are many binary variables. State-of-the-art integer and combinatorial optimization algorithms such as *Branch and Bound and Cutting Plane Methods* may take several hours on a modern workstation to get solutions even for small-scale problems. Our experiments showed that, unfortunately, even an advanced QIP solver such as *CPLEX* from *ILOG* was unable to solve a problem at the size of 100×100 pixels in an acceptable time. Therefore, the main purpose of developing the mixed integer programming model is to identify the global optimal values of some small size problems. We will use them to verify the sub-optimal values generated by other more efficient approaches.

5.2 Error Diffusion. Error diffusion is a classical halftoning technique and is widely used in image process and vision systems. FIGURE 4 shows the basic framework of a typical error diffusion system, where $c(m, n)$ denotes the input continuous-tone, $r(m, n)$ denotes the *rectified* value of the gray-scale pixel, and $b(m, n)$ is the output halftone based on the following equations:

$$r(m, n) = c(m, n) - \sum_{p, q} w(p, q) \cdot e(m-p, n-q) \quad (7)$$

$$b(m, n) = \begin{cases} 1, & \text{if } r(m, n) > t(m, n) \\ 0, & \text{otherwise} \end{cases} \quad (8)$$

The quantizer error $e(m, n)$ is $b(m, n) - r(m, n)$ and $w(p, q)$ is the error weighting matrix, which acts as a low-pass filter. Specially, the sum of the filter matrix is equal to

one to guarantee the stability of the system. A typical filter matrix (Floyd-Steinberg) is also shown in FIGURE 4.

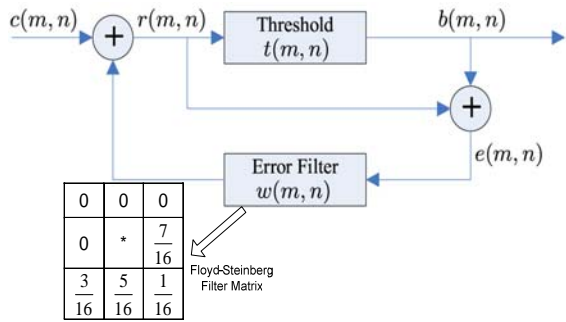


FIGURE 4. ERROR DIFFUSION FRAMEWORK.

5.3 Region based DBS Approach. DBS is an iterative search heuristic which starts with an arbitrary initial halftone and scans through the original image in raster order for changes that can reduce the error. It has been verified that DBS can create high quality halftone images for 2-Dimensional printing [13]. DBS is quite sensitive to the initial halftone. Since screening can generate the bi-level image that can be close to the original continuous-tone image, we employ the screening method with Bayer's matrix to generate the initial halftone for DBS. The commonly used Bayer's matrix is a 8×8 square matrix which has 256 levels. The matrix is periodically tiled on the continuous-tone image to generate the halftone image till visiting all the pixels. Denote $d(m,n)$ as the element of the dither matrix. The screening process can be represented as:

$$b(m,n) = \begin{cases} 1, & c(m,n) \geq d(m,n) \\ 0, & \text{otherwise} \end{cases} \quad (9)$$

Based on the initial halftone image, DBS iteratively visit each pixel as the raster manner to check the perturbation of toggling and swapping. However, the direct evaluation of the objective \mathcal{E} is computationally expensive. We will, therefore, develop an efficient method to evaluate the effect of trial halftone changes. This method relies on the fact that each perturbation of the considered pixel only affects its neighborhood. Thus the error only needs be computed locally. We keep the convolution result $a(x,y)$ and the mean squared error $|a(x,y) - c(x,y)|^2$ for each pixel. After each perturbation, only the terms involved in the

convolution sum that determined $a(x,y)$ should be updated. The related updating formulas are given as follows:

$$\Delta a(x,y) = \sum_{m=0}^{NW} \sum_{n=0}^{NH} \Delta b(m,n) \cdot h(x-m\omega, y-n\omega) \quad (10)$$

$$\Delta |e(x,y)|^2 = [a(x,y) + \Delta a(x,y) - c(x,y)]^2 - [a(x,y) - c(x,y)]^2 = \Delta a(x,y)[2a(x,y) - 2c(x,y) + \Delta a(x,y)] \quad (11)$$

$$a(x,y) \leftarrow a(x,y) + \Delta a(x,y) \quad (12)$$

$$|e(x,y)|^2 \leftarrow |e(x,y)|^2 + \Delta |e(x,y)|^2 \quad (13)$$

For each perturbation, we have one change of $\Delta b(m_0, n_0)$ for toggling or two changes $\Delta b(m_1, n_1)$ and $\Delta b(m_2, n_2)$ for swapping. According to the Equation (5) and Equation (10), for $\Delta b(m_0, n_0)$, only the points in the set \mathcal{S}_0 which are represented as follows has to be changed.

$$\mathcal{S}_0 = \left\{ (x,y) \left| \frac{(x-m\omega)^2}{cw^2} + \frac{(y-n\omega)^2}{ch^2} \leq 1 \right. \right\} \quad (14)$$

The set \mathcal{S}_1 and set \mathcal{S}_2 can be defined in a similar way. Using the parameters defined above, we find only 0.04% of points have to be changed.

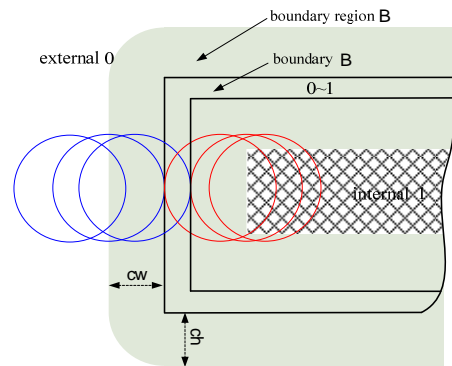


FIGURE 5. BOUNDARY AND BOUNDARY REGION.

We further improve the efficiency of DBS algorithm by utilizing the properties of boundary regions. Layered manufacturing has a unique advantage, that is, we only have to consider the

boundary regions which are often a small portion of a layer. As shown in FIGURE 5, we know that the ratio $c(x, y)$ for the internal portion is "1" and for the external portions is "0". Thus the binary value of the halftone pixels can be calculated separately without further modifications if they have no effects on the boundary regions. For the sake of simplicity, we define two notations, denote B as the boundary set of the image which consists of the pixels with gray scale values between (0, 1), \mathcal{B} as the boundary region of the image, which is the set of pixels around B with the offset distance related to the convolution size (cw, ch) (refer to FIGURE 5 for an illustration). That is, $\mathcal{B} = B \oplus C$, where \oplus denotes the *Minkowski* sum, and C denotes a droplet size. Therefore, a new DBS algorithm based on the boundary region is developed, whose framework is shown as follows.

```

// initialization by screening
1: for each pixel  $(m, n)$  do
2:   if  $c(m, n) \geq d$  ( $m \bmod 8, n \bmod 8$ ) then
3:      $b(m, n) \leftarrow 1$ 
4:   else
5:      $b(m, n) \leftarrow 0$ 
6:   end if
7: end for

// iterative DBS
8: repeat
9:   for each pixel  $(m, n)$  do
10:    if  $(m, n) \in \mathcal{B}$  then
11:      toggle the value of  $(m, n)$ 
12:      evaluate the effect of trial changes by(10-13)
13:      best change  $\leftarrow$  current change
14:      for each pixel  $(p, q) \in \mathcal{S}_{m,n}$  do
15:        if  $(p, q) \in \mathcal{B}$  then
16:          swap  $(m, n)$  and  $(p, q)$ 
17:          evaluate the effect of trial changes
18:          update the best change
19:        end if
20:      end for
21:      update  $|a(x, y) - c(x, y)|^2, b(m, n),$ 
         $a(x, y)$  according to the best change,
        where  $(x, y) \in \mathcal{S}_{m,n}$ 
22:    end if
23:  end for
24: until no changes of  $\mathcal{E}$ 

```

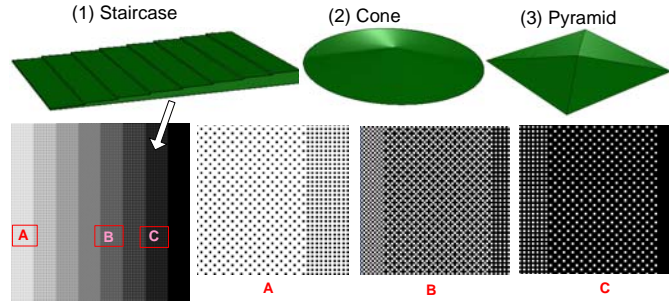


FIGURE 6. CAD MODELS OF THREE SINGLE LAYER CASES WITH THE HALFTONING IMAGE OF STAIRCASE.

6. EXPERIMENTAL RESULTS

A halftoning testbed for the inkjet printing processes has been implemented using C++ programming language with *Microsoft Visual C++* compiler. It can automatically slice an input 3-Dimensional STL model into a set of 2-Dimensional images according to a XY resolution and layer thickness. For each sliced image with gray scale values, a DBS solver can generate a binary halftone image. Based on the droplet layout determined by the image, the testbed will convolute all the droplets and compare the convoluted results with the gray scale image for errors. The same process will be repeated for all the layers to form the solid. Two types of experiments are carried out by using the testbed: (1) we first test single layer cases with different patterns and resolutions; and (2) we then test the approach with 3D CAD models.

6.1 Results for Single Layer Cases. Three single layer cases are shown in FIGURE 6 – top. They are designed for verifying the effectiveness and efficiency of our approach. The x, y sizes of all the models are 1×1 inch. Notice in the staircase pattern, eight different height levels exist within a single layer. Without halftoning technique, a layer thickness that is smaller than each level is required to capture them. In our approach, we can use different halftoning bitmaps to build them all in one layer. The related halftoning bitmaps for some levels are also shown in FIGURE 6 – bottom.

The experimental results for the single layer cases are shown in TABLE 1. As can be seen from the table, the DBS method improves the solution remarkably, while the computation cost is quite reasonable. For the staircase, DBS has much better quality around the side boundary. For the cone and pyramid cases, the surface generated by DBS is much smoother than

screening. As discussed in Section 5.3, the strategy of considering boundary regions can reduce the computational time by around 18%.

TABLE 1. COMPARISON BETWEEN SCREENING, ERROR DIFFUSION AND DBS.

CAD Model	Algorithm	Avg.	Min	Max	SD	CPU (s)
Staircase	Screening	0.025	8.7e-6	2.679	0.075	1.0
	ED	0.024	3.1e-9	2.272	0.066	1.0
	DBS	0.006	1.1e-11	1.043	0.029	180.4
	DBS (with regions)	0.006	1.1e-11	1.043	0.029	150.5
Cone	Screening	0.022	6.1e-10	0.262	0.028	0.8
	ED	0.007	3.1e-12	0.118	0.010	0.8
	DBS	0.004	3.2e-11	0.068	0.006	21.5
	DBS (with regions)	0.004	3.2e-11	0.068	0.006	17.3
Pyramid	Screening	0.022	1.3e-7	0.262	0.031	0.8
	ED	0.009	3.0e-12	0.124	0.012	0.9
	DBS	0.004	3.0e-12	0.090	0.006	36.5
	DBS (with regions)	0.004	3.0e-12	0.090	0.006	31.5

TABLE 2. COMPARISON BETWEEN HALFTONING AND OPTIMIZATION METHODS.

CAD Model	Algorithm	Avg	Min	Max	SD	CPU (s)
Staircase (14x14 pixels)	Screening	0.254	8.7e-6	3.558	0.575	0.02
	DBS	0.119	6.5e-6	1.762	0.272	0.08
	QIP	0.116	1.0e-5	2.201	0.328	35.4
Cone (26x26 pixels)	Screening	0.066	1.9e-7	0.563	0.093	0.02
	DBS	0.010	3.7e-7	0.067	0.011	0.06
	QIP	0.008	5.0e-6	0.036	0.008	46.4
Pyramid (26x26 pixels)	Screening	0.109	4.2e-4	0.548	0.110	0.02
	DBS	0.070	8.3e-5	0.493	0.093	0.05
	QIP	0.057	3.6e-6	0.777	0.123	57.2

A network version of *CPLEX* is also integrated in our testbed. As discussed in Section 5.1, it is very difficult to solve large scale *QIP* model. We only consider some simple cases, i.e., 14×14 pixels for the staircase and 26×26 for the cone and pyramid cases. The result comparison between the halftoning methods and the *QIP* model is listed in TABLE 2. As can be seen from the table, DBS method can find a solution that is very close to the global optimum, while the CPU time is dramatically reduced. For larger cases, the *QIP* solver is unable to find a solution, while DBS can give a good estimate. FIGURE 7 and FIGURE 8 show the comparisons between the computation time and the least squared errors by different methods. Only the simple cases are considered. As can be seen from the figures, the computation cost by *QIP* increases exponentially with the problem scale; while the halftoning methods only consume polynomial time. The solutions obtained by DBS for these

cases are almost the same as the ones obtained by *QIP*. Therefore, we believe DBS can achieve a good balance between effectiveness and efficiency.

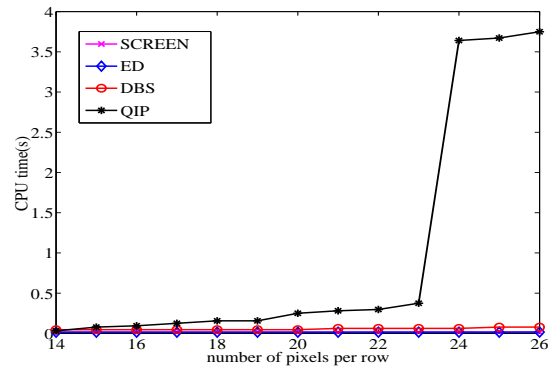


FIGURE 7. COMPARISON OF COMPUTATION COST.

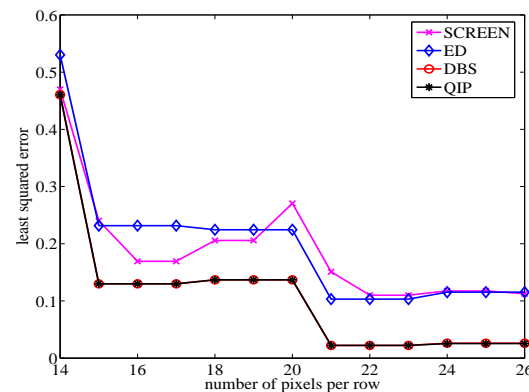


FIGURE 8. COMPARISON OF LEAST SQUARED ERRORS.

6.2 Results for Solid Cases. In addition to simple geometries such as cone, pyramid and spherical cap, we also use the testbed to test various 3D CAD models. The layer thickness are set at a value that is much bigger than those required by traditional methods. A test case is shown in FIGURE 9. A thick layer of an input model is taken from two slicing planes, Z_1 and Z_2 . The halftoning images generated by DBS are also shown in the figure. We can see the boundary regions built by the halftoning images are much smoother than the ones built by the traditional methods. We plan to further test the relations between layer thickness and surface quality to understand the limit for the productivity improvement of the inkjet printing processes.

7. CONCLUSION AND FUTURE WORK

A 3-dimensional digital halftoning method has been developed for the layered based inkjet

printing processes. Droplets are intelligently controlled to form a slanted layer which can closely match the surface of the input geometry. Therefore, a significantly less number of layers will be required for an input geometry. It will consequently reduce the building time. To generate an optimized droplet layout, we mathematically define the halftoning problem for 3D inkjet printing. We also explore various solution strategies including the adaptation of screening, error diffusing, a region based DBS, and a quadratic integer optimization model. The experimental results show that the region based DBS method can solve the test cases effectively and efficiently.

Future research work includes physical experiments by using an inkjet printing machine. This requires the integration of our droplet planning results into the controller module of the printing machine. Based on it, designed experiments will be performed on droplet accumulation effects and quantitative measurements will be compared with our simulation results. We also plan to integrate the adaptive slicing scheme into our halftoning method to further improve the productivity of the inkjet printing processes.

REFERENCES

- [1] Kulkarni, P.M. (1998), "Process planning for the layer domain of layered manufacturing", Ph.D. Dissertation, The University of Michigan.
- [2] Hope, R.L, P.A. Jacobs, R.N. Roth (1997), "Rapid prototyping with sloping surfaces", Rapid Prototyping Journal, Vol.3, No. 1, pp. 12-19.
- [3] Amon, C. H., J.L. Beuth, L.E. Weiss, R. Merz, and F.B. Prinz (1998), "Shape deposition manufacturing with microcasting: processing thermal and mechanical issues", Journal of Manufacturing Science and Engineering, Vol. 120, No. 3, pp. 656-665.
- [4] Khoshnevis, B. (2004), "Automated construction by contour crafting," Journal of Automation in Construction, vol. 13 (1), pp. 5-19.
- [5] Horvath, I. and J. S. M. Vergeest, "Finding the shape of flexible blade for freeform layered manufacturing of plastic foam objects", Proceedings of DETC'98, Atlanta, September 13-16, 1998.

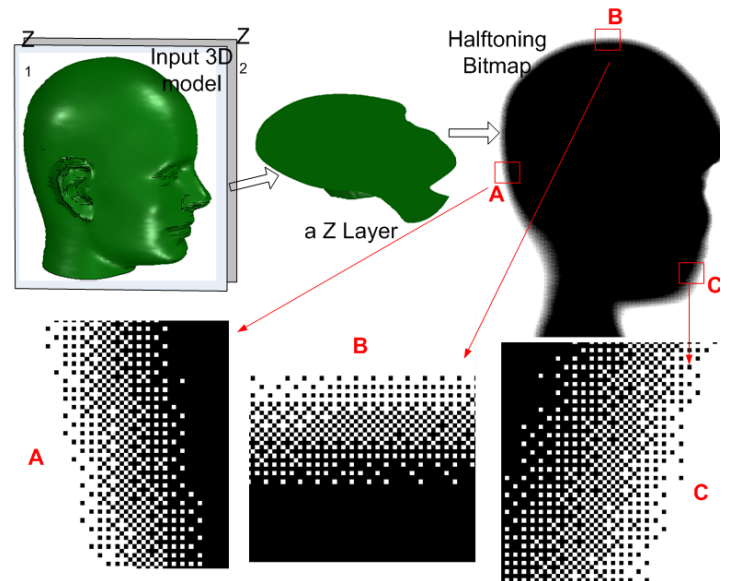


FIGURE 9. CAD MODEL OF A SOLID CASE WITH THE HALFTONING IMAGE.

- [6] Ulichney, R. (1987). "Digital halftoning," MIT Press.
- [7] Bayer, B.E. (1973). "An optimum method for two level rendition of continuous-tone pictures." in Proc. IEEE Int. Conf. Commun., Conf. Rec., pp. 2611-2615.
- [8] Floyd, R.W. and L. Steinberg (1976). "An adaptive algorithm for spatial greyscale," Proc. Soc. Inf. Disp., vol. 17, no. 2, pp. 75-77.
- [9] Analoui, M. and J. Allebach (1992). "Model-based halftoning using direct binary search." in Proceedings of SPIE, vol. 1666, (San Jose CA), pp. 96-108.
- [10] Cho, W., E. M. Sachs, N. M. Patrikalakis, and D. E. Troxel (2003), A dithering algorithm for local composition control with three-dimensional printing, Computer-aided Design, Vol. 35, pp.851-867.
- [11] Le, H. P (1998), Progress and Trends in Ink-jet Printing Technology, Journal of Imaging Science and Technology, Vol. 42, No. 1.
- [12] Bao, Z. (2004), Conducting polymers: fine printing, Nature Materials, Vol. 3, pp. 137-138.
- [13] Lieberman, D. and J. P. Allebach (1997). "Efficient model based halftoning using direct binary search," in Proc. 1997 IEEE Int. Conf. Image Processing, Santa Barbara, CA.